

Holographic recording and beam coupling in ferroelectric $\text{Bi}_4\text{Ti}_3\text{O}_{12}$

X. Yue, F. Mersch, R. Rupp, U. Hellwig, and M. Simon

Fachbereich Physik der Universität Osnabrück, D-49069 Osnabrück, Germany

(Received 6 November 1995)

Holographic gratings were recorded in a ferroelectric bismuth titanate crystal. Refractive index as well as absorption gratings contribute to the recording process with modulation amplitudes $\Delta n = 1.8 \times 10^{-5}$ and $\Delta \alpha = 0.8 \text{ cm}^{-1}$, respectively. The dominating charge transport mechanism for the formation of the space-charge field in the crystal is diffusion. The dependence of the photorefractive gain on the writing crossing angle and thus the effective photorefractive charge density of our sample was determined by beam-coupling experiments.

I. INTRODUCTION

Bismuth titanate ($\text{Bi}_4\text{Ti}_3\text{O}_{12}$) is one of the bismuth compounds with a layer structure of oxygen octahedra. It has interesting electro-optical properties, i.e., it has an a -axis component as well as a c -axis component of remanent polarization and exhibits different orientations of the optical indicatrix corresponding to two states of remanent polarization, which makes it useful in optical memory and display applications.¹ In the past, it was extensively studied for ferroelectric optical memory devices.^{2,3} But up to now there is no report on the photorefractive properties of this crystal to our knowledge. In this paper we report our experimental studies on holographic recording and beam coupling in $\text{Bi}_4\text{Ti}_3\text{O}_{12}$. This is the first time, to our knowledge, that holographic recording employing the photorefractive effect in this material has been realized. There are several reasons why we chose this crystal for our experiments. (1) At room temperature this crystal is in a ferroelectric monoclinic phase with the symmetry of point group m , in contrast to most other popular photorefractive crystals which possess higher symmetries such as $4mm$ (BaTiO_3 , SBN) or $3m$ (LiNbO_3). To date there are only scarce reports on photorefractive materials with monoclinic symmetry. Examples are triglycine sulfate (TGS) (Ref. 4) and $\text{Sn}_2\text{P}_2\text{S}_6$.⁵ (2) There are more than 60 compounds in the Aurivillius family which have layered-structure perovskite phases and most of them are ferroelectric like $\text{Bi}_4\text{Ti}_3\text{O}_{12}$,⁶ so that the study of this crystal may give some important clues in the search for new photorefractive materials.

II. EXPERIMENTAL METHODS

The $\text{Bi}_4\text{Ti}_3\text{O}_{12}$ sample used in our experiment was grown using modified Nacken-Kyropoulos technique at our university. The dimension of the sample is $0.76 \times 4.65 \times 7.90 \text{ mm}^3$. The orientations of the axes are shown in Fig. 1(a). The sample is cut with respect to the paraelectric phase and almost completely poled to single domain. The extinction spectrum is shown in Fig. 2, in which the reflections of the surfaces have been accounted for.

The usual experimental configurations for holographic recording and two-wave mixing were employed in our experiments.⁷ An Ar^+ laser operated in the TEM₀₀ mode at

a wavelength of 514.5 or 488 nm and the polarization of its output beam was controlled by a half-wave plate. In the holographic experiment, one of the writing beams was used also as the readout beam by simply blocking the other writing beam. We define the diffraction efficiencies as $\eta_1 = I_{1d}/(I_{1t} + I_{1d})$ (beam 2 blocked) and $\eta_2 = I_{2d}/(I_{2t} + I_{2d})$ (beam 1 blocked), where $I_{1,d}$ and $I_{1,t}$ are the diffracted and transmitted intensities of beams I_1 and I_2 , respectively. The notations for the beams are shown in Fig. 1(b).

III. EXPERIMENTAL RESULTS

In the first experiment we chose the polarization of both incident beams along the horizontal or vertical direction and defined the angle between grating vector and the b axis as Φ . By rotating the crystal around the c axis, the measured diffraction efficiency (η_1) is shown in Fig. 3 as a function of Φ . It can be seen from this figure that the maximum value of η_1 occurs when the grating vector is along the a axis and the polarization of both beams lies in the plane of incidence. In the subsequent experiments we used this geometry of maximum efficiency.

The time dependence of holographic recording and erasure in this sample is shown in Fig. 4. The remarkable difference between η_1 and η_2 indicates, according to Ref. 8, that refractive-index and absorption gratings with a phase

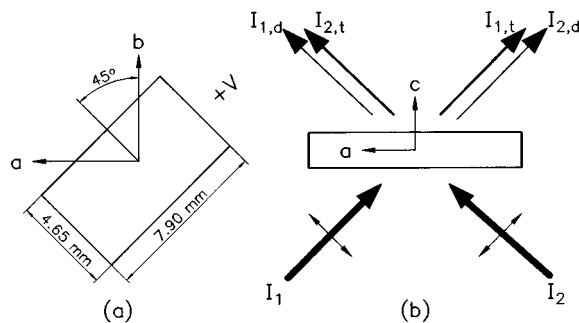


FIG. 1. Crystal orientation (a) and experimental arrangement (b). +V denotes the positive electrode for poling. The angle of the b axis to the 4.65 mm long edge is 40° . Beams 1 and 2 have the same polarization lying in the plane of incidence.

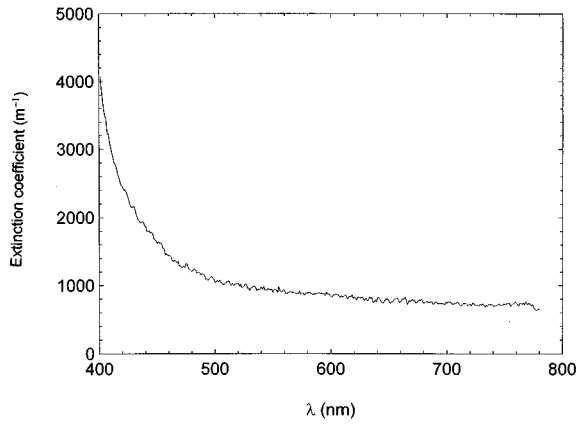


FIG. 2. Extinction spectrum of the sample used at room temperature taking reflection losses into account.

shift with respect to each other are present in this crystal.

In order to prove this conclusion, we shifted the crystal along the grating vector with a piezoelectric transducer at a speed much faster than the holographic grating response after the grating was written in the crystal.^{7,9} The changes of both output intensities as a function of the shift of the crystal are shown in Fig. 5. It can be clearly seen that the intensity changes of both beams have opposite phase and different amplitudes, which indicates that refractive-index as well as absorption gratings coexist. As described by Sutter and Günter,⁹ if the translation time is much shorter than the time needed to build up a new grating, and under the condition that the diffraction efficiencies are small, the sum [$I_+(x)$] and the difference [$I_-(x)$] of the intensities of both interacting beams ($I^{(1)}$ and $I^{(2)}$) behind the crystal can be written as

$$I_+(x) = I^{(1)} + I^{(2)} = I_0 \exp(-\alpha d / \cos\theta) [2 - 4a \cos(\phi_a + 2\pi x / \Lambda)], \quad (1)$$

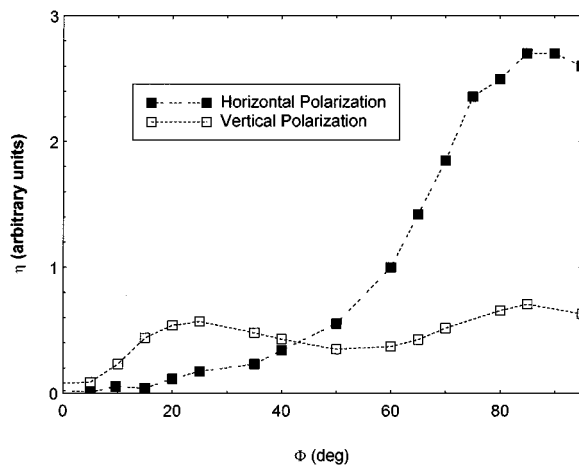


FIG. 3. Measured diffraction efficiency η_1 at different angles Φ (Φ is the angle between grating vector and b axis) for horizontal and vertical polarizations.

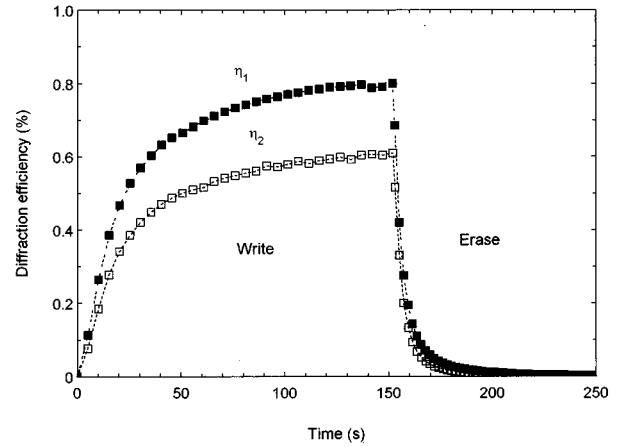


FIG. 4. Write-erase cycle of the sample used. Here η_1 and η_2 denote the diffraction efficiencies as defined in the text.

$$I_-(x) = I^{(1)} - I^{(2)} = I_0 \exp(-\alpha d / \cos\theta) [-4p \sin(\phi_p + 2\pi x / \Lambda)], \quad (2)$$

where Λ is the grating spacing, I_0 the incident intensity, and θ the half crossing angle between both writing beams inside the crystal. $I_+(x)$ and $I_-(x)$ oscillate with relative amplitudes $4a$ and $4p$ which are related to the absorption and refractive-index modulations $\Delta\alpha$ and Δn , respectively:

$$p = \frac{\pi \Delta n d}{\lambda \cos\theta}, \quad a = \frac{\Delta \alpha d}{4 \cos\theta}. \quad (3)$$

Here ϕ_p and ϕ_a are the phase shifts of the refractive-index and the absorption gratings with respect to the intensity pattern, respectively. By recording I_+ and I_- as a function of grating translation x , the phase shift as well as amplitude of the refractive-index and absorption gratings can be determined. Using this technique we measured the mean values $\phi_p \approx 90^\circ$ and $\phi_a \approx 0^\circ$ for the phase shifts of these two gratings and determined also that the saturated refractive-index modulation is about 5.8×10^{-6} , and the absorption modula-

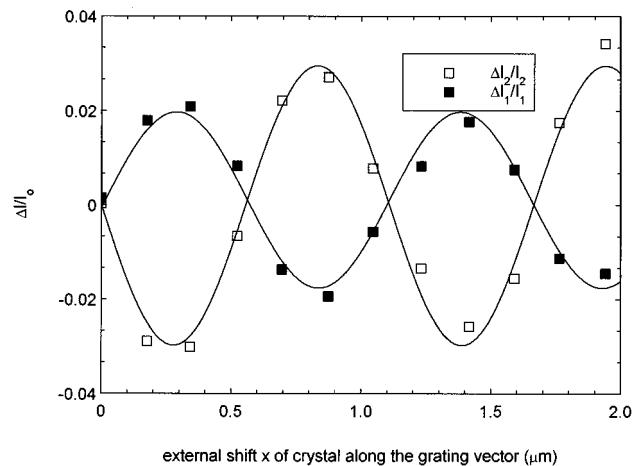


FIG. 5. Changes of both output intensities as a function of the external shift of the crystal along the grating vector.

tion is about 0.3 cm^{-1} under the following experimental conditions: $\lambda = 514.5 \text{ nm}$, $\Lambda = 1.2 \text{ }\mu\text{m}$, and an intensity of 0.5 W cm^{-2} . Because of reflection and extinction losses the intensities of the beams at the output surface are decreased to about 28% ($\lambda = 488 \text{ nm}$, 25%) of their original values.

Unfortunately, because of a lack of mechanical resolution in the piezoelectric transducer, it is difficult to obtain the corresponding information when the grating spacing is small. But based on the above measurement, we assumed that the dephasing of both gratings is 90° and measured η_1 and η_2 at various conditions. From the result in Ref. 8 we obtain η_1 and η_2 when the diffraction efficiencies of both gratings are very small:

$$\eta_{1,2} = \left(\frac{\pi d}{\lambda \cos \theta} \right)^2 [(\Delta n)^2 + (\Delta \kappa)^2 \pm \Delta n \Delta \kappa], \quad (4)$$

where $\Delta \kappa = \Delta \alpha \lambda / 2\pi$ is regarded as an effective absorption index change.

In the experiments we first recorded the rise of η_1 and η_2 . (We recorded both curves separately under the same conditions. The results were reproducible with an accuracy better than 4%.) We then calculated Δn and $\Delta \kappa$ according to the above equations. It is found that the maximum modulations of refractive and absorption indices are $\Delta n = 1.8 \times 10^{-5}$ and $\Delta \kappa = 6.6 \times 10^{-6}$, respectively, for a grating spacing of $0.5 \text{ }\mu\text{m}$ and a wavelength of 514.5 nm . Clearly, the absorption-index modulation corresponding to a change $\Delta \alpha = 0.8 \text{ cm}^{-1}$ of the absorption constant in this condition is much smaller than the refractive index modulation; that means that the refractive-index grating dominates in the holographic recording. The measured diffraction efficiency η_1 under this condition is about 1.12%.

We also measured the time constant τ for dark decay of the refractive grating with this method. Under the same condition as described above, the measured dark decay time constant is $\tau = 76 \text{ s}$. From $\tau = \epsilon \epsilon_0 / 4\pi \sigma_d$ and with $\epsilon = 120$,¹⁰ we obtained for the dark conductivity $\sigma_d = 1.1 \times 10^{-12} \text{ (}\Omega \text{ m)}^{-1}$.

From the above experimental result on the phase shift of the refractive-index grating with respect to the intensity pattern, we know that diffusion of photoinduced charges is the main transport mechanism which is responsible for the photorefractive effect in $\text{Bi}_4\text{Ti}_3\text{O}_{12}$. This indicates also that there should be an energy exchange for two-wave mixing without application of an electric field to the crystal.

In our two-waving mixing experiment we chose a beam ratio I_1/I_2 of about 200. Energy is always transferred towards the positive a axis, which is defined here as the direction towards the negative electrode applied for poling. Because coupling is not very strong and depletion of the strong beam is negligible, the beam-coupling gain can be defined as

$$\Gamma = \frac{1}{d} \ln \left(\frac{I_2(\text{ with pump beam})}{I_2(\text{ without pump beam})} \right). \quad (5)$$

Its dependence on the crossing angle between both interacting beams was measured and is shown in Fig. 6 in which the solid curve is the best fit to the relationship:¹¹

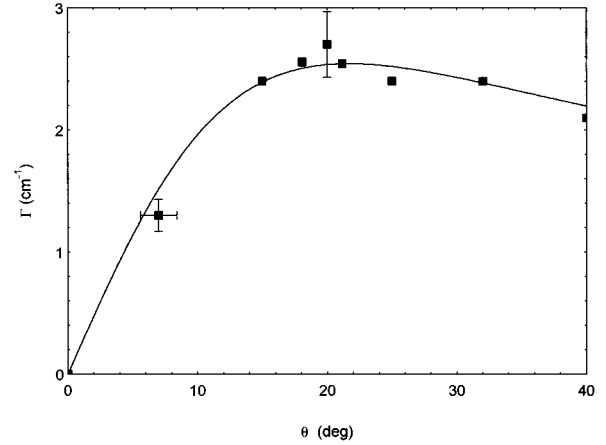


FIG. 6. Two-beam coupling gain as a function of half of the external crossing angle.

$$\Gamma = \frac{2\pi}{\lambda} \frac{r_{\text{eff}}}{n \cos \theta} \frac{k_B T}{e} \frac{K}{1 + (K/K_D)^2}, \quad (6)$$

where r_{eff} is the effective electro-optic coefficient, $K = 2\pi/\Lambda$, and K_D is the inverse Debye screening length which is defined as

$$K_D = \sqrt{e^2 N_{\text{eff}} / (\epsilon \epsilon_0 k_B T)}. \quad (7)$$

With the value $K_D = 8.3 \times 10^6 \text{ m}^{-1}$ from the best fit, we obtain the effective density $N_{\text{eff}} = 1.2 \times 10^{16} \text{ cm}^{-3}$ of photorefractive centers. From the fit to the experimental data we also obtain an effective electro-optic coefficient of about 7.8 pm/V assuming that there is no electron-hole competition. The maximum gain obtained is 2.8 cm^{-1} for a wavelength of 514.5 nm and grating spacing $\Lambda = 0.75 \text{ }\mu\text{m}$.

It should be emphasized that the present work is targeted on an optical storage principle which is different from the ferroelectric optical memory device reported in the past, because there is no applied electric field in either the writing or reading process to reverse the component of polarization. It is clear that the refractive-index grating is caused by the light-induced space-charge field, which modulates the refractive index via the linear electro-optic effect. But the mechanism for the absorption grating is not known yet. In the present experiment we failed to find the exact formation regularity of the absorption grating. Generally speaking, its magnitude changes with the variation of the crossing angle and its response time is of the same order as the photorefractive response, but both gratings are phase shifted by $\pi/2$ with respect to each other. It seems that the photochromic grating which is produced by periodically ionized deep-level and free-carrier distributions is responsible for the modulation of absorption.¹² Further experiments with $\text{Bi}_4\text{Ti}_3\text{O}_{12}$ crystals with better optical quality need to be conducted to find the mechanism responsible for this absorption grating.

Because the present sample was cut with respect to the paraelectric phase, many fundamental photorefractive parameters of this crystal cannot be characterized. But the present experiments have shown clearly that this crystal has some interesting photorefractive properties, for example, with such a partially poled sample, a moderate photorefractive gain was measured, and with diffusion as the dominating charge

transport mechanism, it has the optimal phase shift between the refractive-index grating and intensity pattern for beam coupling. Photorefractive properties of this material might still be optimized by proper doping.

IV. CONCLUSION

We reported experimental results on holographic recording and beam coupling in the ferroelectric crystal $\text{Bi}_4\text{Ti}_3\text{O}_{12}$. Both a photorefractive and an absorption grating contribute to the measured diffraction efficiency of more than 1%. The photorefractive grating is dominated by diffu-

sion of free carriers which are responsible for the formation of the space-charge field. There is an energy exchange between the two interacting beams without application of an electric field and the beam coupling gain is about 2.8 cm^{-1} .

ACKNOWLEDGMENTS

We thank B. Sugg for his assistance in the experiments. Financial support by the Deutsche Forschungsgemeinschaft (SFB 225, A6) and Friedrich Ebert-Stiftung are gratefully acknowledged.

¹Y. Xu, *Ferroelectric Materials and their Application* (Elsevier Science Publisher B.V., Amsterdam, 1991).

²S. A. Keneman and A. G. W. Taylor, *Ferroelectrics* **1**, 227 (1970).

³S. A. Keneman, A. Miller, and G. W. Taylor, *Appl. Opt.* **9**, 2279 (1970).

⁴G. Montemezzani, J. Fousek, J. Hulliger, and P. Günter, *Ferroelectrics* **126**, 103 (1992).

⁵S. G. Odoulov *et al.*, *Opt. Lett.* (to be published).

⁶Y. Masuda *et al.*, *Jpn. J. Appl. Phys.* **31**, Pt. 1B, 3108 (1992).

⁷R. A. Rupp, A. Maillard, and J. Walter, *Appl. Phys. A* **49**, 259 (1989).

⁸E. Guibelalde, *Opt. Quantum Electron.* **16**, 173 (1984).

⁹K. Sutter and P. Günter, *J. Opt. Soc. Am. B* **7**, 2274 (1990).

¹⁰A. Fouskova and L. E. Cross, *J. Appl. Phys.* **41**, 2834 (1970).

¹¹M. D. Ewbank, R. R. Neurgaonkar, W. K. Cory, and J. Feinberg, *J. Appl. Phys.* **62**, 374 (1987).

¹²R. B. Bylisma, D. H. Olson, and A. M. Glass, *Opt. Lett.* **13**, 853 (1988).